Experimental and theoretical investigation of γ-butyrolactone decomposition on lithium electrode surface. Effect of Li_3N layer

O. V. Yarmolenko, G. Z. Tulibaeva, G. N. Petrova, A. F. Shestakov, N. I. Shuvalova, V. M. Martynenko, and O. N. Efimov*

Institute of Problems of Chemical Physics of the Russian Academy of Sciences, 1 prosp. Akad. Semenova, 142432 Chernogolovka, Moscow Region, Russian Federation. Fax.: +7 (496) 522 5625. E-mail: oyarm@icp.ac.ru

Dependence of gassing upon decomposition of 1 *M* $LiClO_4$ electrolyte in γ-butyrolactone (γBL) with various contents of water (0.008 and 0.2% w/w) at a lithium electrode on the current density of charging was studied. Quantum chemical modeling of γBL interaction with lithium surface was performed. The initial stage of γBL decomposition is the formation of a surface organolithium compound, which is hydrolyzed in the subsequent reactions with water.

Key words: γ-butyrolactone, lithium electrode, lithium nitride, gassing, quantum chemical modeling, density functional theory.

Lithium batteries are fairly promising electrochemical power sources. However, there is a number of problems brought about by deterioration of the lithium—electrolyte interface with time. First, cycling in organic electrolytes is accompanied by side corrosion reactions of lithium metal and decomposition of electrolyte components to give gaseous products, which increase the pressure inside the electrochemical cell. Second, dendrite formation creates conditions for short-circuit failure on the lithium electrode surface.

The problem of passivation of the lithium electrode surface in organic electrolytes has been known since the 1970s.[1] Thermodynamic calculations indicate that lithium reduces aprotic polar solvents used in lithium batteries.[2] For a number of solvents (ethylene carbonate, propylene carbonate, ethyl methyl carbonate, dimethyl carbonate, *etc*.), the reactions with lithium and the composition of the surface layers have been studied rather comprehensively.[2,3] On going from pure solvents to electrolytes, the electrolyte salt also becomes involved in the construction of surface layers together with the solvents.[2,3] Only some compounds do form a surface layer on lithium in different solvents and electrolyte solutions. The inorganic compounds that refer to this type include the oxide Li_2O, hydroxide LiOH, carbonate Li_2CO_3, chloride LiCl, fluoride LiF, dithionite $Li_2S_2O_4$, carbide Li_2C, and nitride Li_3N. Among organic compounds, lithium methoxide and butoxide with the formula ROLi should be mentioned.[2,3] Electrolyte decomposition processes and compositions of the surface layers have been studied in a number of works.[4—19]

On lithium contact with many gases (including dry O_2 and CO_2), organic and inorganic solvents, and solutions on the metal surface, a passive protective film is formed, representing a layer of insoluble products formed in the reaction of lithium with the environment.[20] This is a continuous, non-porous, 1—100-nm thick layer having low electronic conductivity, which retards the redox processes involving the electrolyte. Meanwhile, the formation of the insulating layer does not deprive lithium of the electrochemical activity. While functioning as the negative electrode in contact with an electrolyte, lithium is dissolved at a rather high rate (at a current density of up to 0.1 and even 0.5—1.0 mA cm^{-2}) without disruption of the passive layer. Hence, the layer material possesses electrical conductivity of lithium ions, thus functioning as a lithium-conducting ionic conductor or solid electrolyte.

The purpose of this work is experimental and theoretical study of γ-butyrolactone (γBL) decomposition on the surface of a lithium electrode during charging with lithium electrode potential shift to negative region.

The reaction of γBL with alkali metals was studied previously.[2,3] It is known[2] that lithium cutting under a γBL layer produces a short gas pulse after which the surface is passivated; however, gas release on sodium or potassium is more prolonged. The gases were found[2] to contain methane and C_2, C_3, and C_4 hydrocarbons. In the absence of gassing in moist γBL, the salt $LiO(CH_2)_3COOLi$ was found.[3]

The effect of coating the lithium electrode by a thin layer of lithium nitride, which functions as ionic conduc-

Published in Russian in *Izvestiya Akademii Nauk. Seriya Khimicheskaya,* No. 3, pp. 500—506, March, 2010.

1066-5285/10/5903-0510

tor with a conductivity of $(2—4) \cdot 10^{-4}$ Cm cm^{-1} at 20 °C, on the decomposition of 1 *M* $LiClO_4$ electrolyte in γBL in the presence of 0.2% (w/w) water was studied.[21]

Studies of the composition and formation mechanism of the gaseous products in the reaction of the lithium electrode surface with 1 *M* $LiClO_4$ in γBL in the presence of water is of considerable practical value, as the manufacturers of lithium ion batteries are always faced with the problem of unsuitability of a wet electrolyte.

Experimental

A 1 *M* $LiClO_4$ electrolyte in γBL (LLC Ecotech, Chernogolovka) with a water content of 0.008% (w/w) was used. The side electrolyte decomposition reactions were studied by introducing 0.2% (w/w) of water.

Lithium electrodes were manufactured using a 120 μm Ni grid (inert toward the electrolyte studied). A 2-mm thick lithium metal foil was pressed onto the grid; the surface area was 1 cm^2. All operations with lithium metal were carried out in an argon glove box.

To obtain the lithium nitride coating, a lithium electrode was placed in an ampoule and evacuated, and high-purity nitrogen was let in under atmospheric pressure. The ampoule with the lithium electrode in a nitrogen atmosphere was kept at 100 °C until a black-colored coating appeared on the lithium surface (2—4 h).

To determine the amount of nitrogen on the surface, the lithium electrode was dissolved in 0.1 *M* HCl (special purity grade). The ammonium salts thus formed were converted to ammonia on refluxing in 40% alkali, the ammonia being steam-distilled off into 0.01 *M* acid, and this solution was analyzed by means of phenol and sodium hypochlorite (indophenol method of nitrogen analysis[22]). The nitrogen content in the lithium surface layer was $\sim 7.8 \cdot 10^{-4}$ mol, which corresponds to a 0.125-mm thick lithium nitride layer.

The release of gaseous products of 1 *M* $LiClO_4$ electrolyte decomposition in γBL was studied in the galvanostatic mode on a P-5827M potentiostat at a current density of 0.5, 1.0, 1.5, and 2.0 mA cm^{-2} in a three-electrode cell (Fig. 1) at 20 °C. A standard silver chloride electrode was used as the reference electrode; it was separated from the electrolyte by an electrolytic bridge filled with the same electrolyte. Platinum metal served as the counter electrode. The cell was connected to a vacuum circulation setup with argon (special purity grade) being continuously pumped through the closed circuit during the electrolysis. The argon pressure in the setup was higher than atmospheric pressure by ~10 Torr in order to avoid air inflow from the atmosphere. The contents and the composition of the hydrocarbons evolved during the electrolysis were analyzed by taking samples by means of the multiway valve, the samples being supplied to a Biokhrom chromatograph with Al_2O_3-packed columns (0.4×300 cm) and a flame ionization detector.

The gas phase was additionally analyzed by mass spectrometry to determine the content of hydrogen and oxygen compounds. Mass spectrometric analysis was carried out using a MI 1201V mass spectrometer. The gas phase was sampled at the end of the experiment.

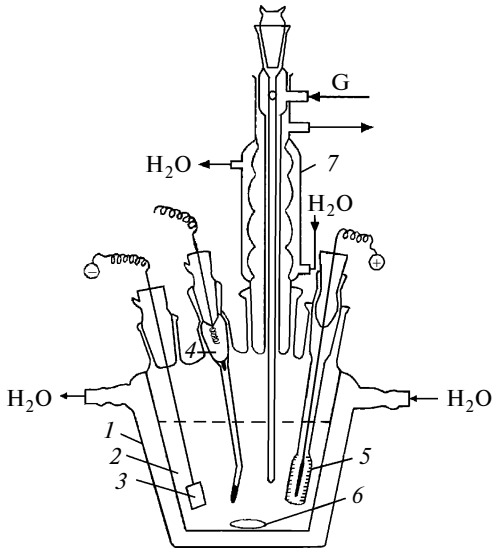

Fig. 1. Draft view of the electrochemical cell: (*1*) thermostated cell, (*2*) organic liquid electrolyte, (*3*) working Li electrode, (*4*) reference electrode $Ag^+/AgCl$, (*5*) Pt counter electrode, (*6*) magnetic stirrer, (*7*) reflux condenser, G is gas.

Results and Discussion

Gasification as a result of decomposition of wet 1 *M* $LiClO_4$ electrolyte in γBL was studied in the galvanostatic mode. This electrolyte with a water content of 0.008% w/w does not decompose at a pure lithium electrode even when the current density increases to 2.0 mA cm^{-2}.

At a pure lithium electrode and current densities of 0.5 and 1.0 mA cm^{-2}, γBL does not decompose in the presence of 0.2 mol.% of water, while at current densities of 1.5 and 2.0 mA cm^{-2}, five gaseous hydrocarbons are evolved, the release rate and the product ratio being varied upon change in the current density (Fig. 2). The products include both saturated (C_3H_8, C_2H_6, CH_4) and unsaturated hydrocarbons (C_3H_6, C_2H_4) but no C_4 hydrocarbons.

When the current density is 1.5 mA cm^{-2}, ethane is the major product of electrolysis, the yields of other products increasing in the sequence $CH_4 = C_3H_6 < C_3H_8 < C_2H_4 < C_2H_6$ (Table 1, see Fig. 2). For a current density of 2.0 mA cm^{-2}, the initial rates of hydrocarbon formation increase 1.5—6.6-fold and a different product ratio is observed, namely,: $CH_4 < C_3H_6 < C_2H_4 < C_2H_6 < C_3H_8$. Changes in the product yields are much more pronounced than the increase in the current density, indicating a considerable effect of electrochemical processes. Moreover, the properties of the lithium surface change with time at a constant current density (1.5 mA cm^{-2}), as follows from the kink on the kinetic curve of ethylene formation. Note that the experiments were carried out at one and the same electrode with successive increase in the current density.

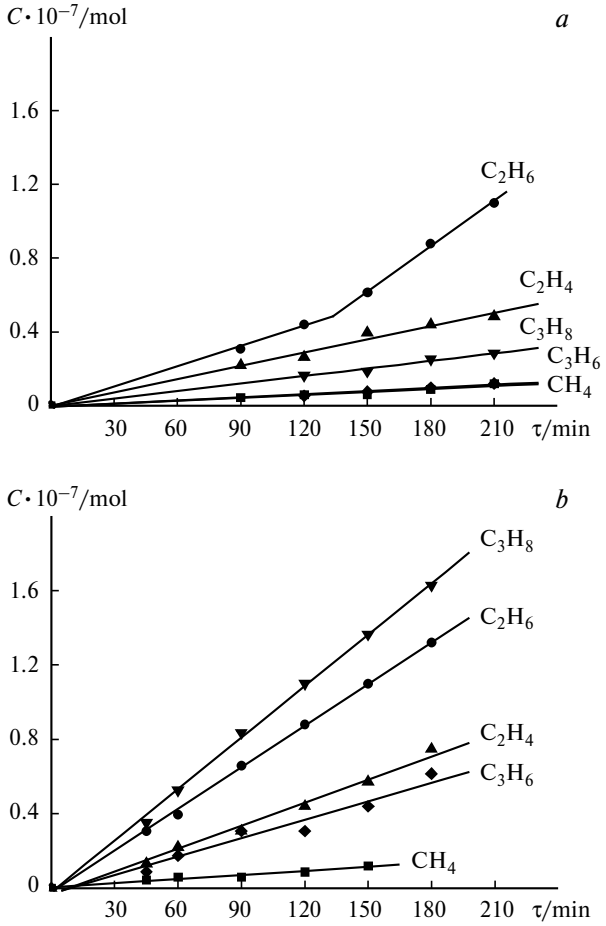

Fig. 2. Decomposition of wet 1 *M* $LiClO_4$ electrolyte in γBL at a Li electrode at current densities of 1.5 (*a*) and 2.0 mA cm^{-2} (*b*).

With allowance of the CO and CO_2 impurities, the mass spectra of the gas phase (Fig. 3) show the presence of H_2, CO, and CO_2 in the initial argon manifested as H_2^+ (*m*/*z* 2), CO^+ (*m*/*z* 28), and CO_2^+ (*m*/*z* 44) peaks. From the mass spectrum of the gas-phase product mixture, the peaks for the carrier gas (Ar, *m*/*z* 40 and 20) were removed for the sake of clarity. It also follows from Fig. 3 that the hydrocarbons already detected by chromatography are not manifested in the mass spectra. However, by using the

Table 1. Decomposition rate of wet 1 *M* $LiClO_4$ electrolyte in γBL at a lithium electrode

Current density /mA cm^{-2}	Gasification rate·10^{10} /mol min^{-1} cm^{-2}				
	CH_4	C_2H_4	C_2H_6	C_3H_6	C_3H_8
1.5	0.53	2.4	3.6/8.1*	0.57	1.4
2.0	0.73	4.1	7.4	3.30	9.2

* The values correspond to the initial/end segment of the kinetic curve.

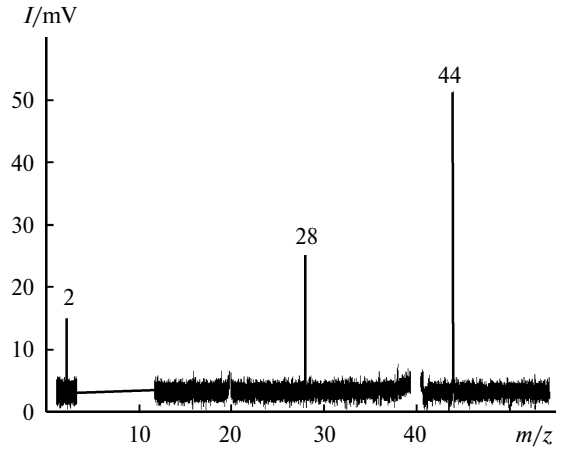

Fig. 3. Mass spectra of the reaction products in the gas phase.

accumulation procedure and enrichment of the gaseous electrolysis products through condensation at liquid nitrogen temperature, the hydrocarbons CH_4, C_2H_4, and C_2H_6 and the alcohols MeOH and Pr^iOH were detected in the condensate mass spectra apart from H_2, CO, and CO_2. Figure 4 shows the mass spectrum of the condensate where the peaks with *m*/*z* = 28 and 44 are somewhat reduced in height for better display of the minor peaks, while Table 2 presents the same mass spectrum with peak assignment to particular chemical compounds.

The composition of the condensate reflects only qualitatively the composition of the electrolysis products, as the quantitative ratio of the components may differ from that in the gas phase. The contents of methane and higher hydrocarbons in the condensate are comparable, whereas in the gas phase methane is a minor product. The condensate mass spectrum exhibits also methyl and isopropyl alcohols. It is clear that such polar liquids would be the first to condense in the liquid nitrogen trap. As a consequence, despite the similar intensities of the hydrocarbon and alcohol peaks in the mass spectrum of the condensate, the content of the latter in the gas phase is substantially

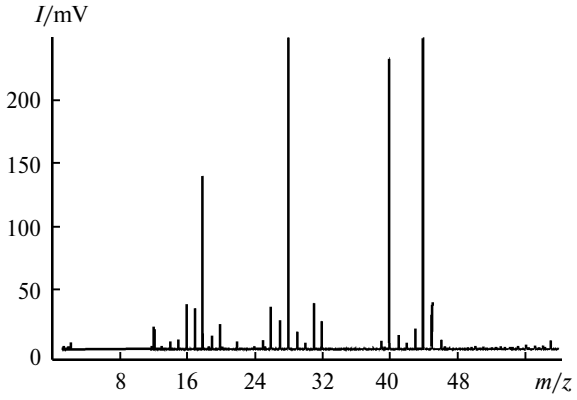

Fig. 4. Mass spectra of the condensate of the reaction products.

lower. This is why they cannot be detected in the gas chromatographic analysis. However, the alcohols can be accumulated to a larger extent in solution. For this reason, the actual hydrocarbon and alcohol ratio in the γBL decomposition products was not determined.

When the lithium electrode is replaced by a nitrogen-treated lithium electrode, no gaseous γBL decomposition products were found at a current density of up to 2.0 mA cm^{-2}. Thus, the Li_3N layer is a protective coating for lithium metal.

Theoretical analysis of the γBL decomposition mechanism. Experimental data indicate that the current density affects considerably both the gassing rate and the composition of the electrolysis products (see Tables 1 and 2). It is also known[23] that there exist some current density limit after which fast dendrite growth on the lithium surface starts.

For elucidating the reasons for change in the gas composition, the knowledge of fina structural features of the surface of growing lithium electrode is required but currently no such knowledge is available. Therefore, the task was to establish only the key features of the reaction of γBL solvent molecule with the Li surface. The surface active sites were modeled by Li_{20} clusters. The interaction of γBL molecule with the Li_{20} cluster was studied by the quantum chemical density functional theory method. The *ab initio* PBE functional[24] and the extended basis set H [6s2p/2s1p], C, O [10s7p3d/3s2p1d], Li [10s7p3d/4s3p1d] were used. All calculations were carried out using the PRIRODA program package.[25] This approach made it possible to describe satisfactorily the structure and the relative energies of isomers of the Li_6 cluster for which the results of high-precision computation are available[26] and for the γBL molecule.[27]

Table 2. Mass spectra of the condensate of the reaction products

m/z	I_{rel} (%)	Assignment*
2	1.4	$[H_2]^+$
12	3.8	$[C]^+$
13	1.0	$[CH]^+$
14	1.6	$[CH_2]^+$
15	1.8	$[CH_3]^+$, (CH_4O), (CH_4)
16	6.9	$[CH_4]^+$, (CH_4), $[O]^+$, (CO), (CO_2)
17	6.4	$[HO]^+$, (H_2O)
18	25.2	$[H_2O]^+$, (H_2O)
20	4.1	$[Ar]^{++}$
22	1.6	$[CO_2]^{++}$
25	1.8	(C_2H_6), (C_2H_4)
26	6.6	(C_2H_6), (C_2H_4)
27	4.7	(C_2H_4), (C_2H_6), (C_3H_6)
28	63.0	$[CO]^+$, (CO), (C_2H_6)
29	3.1	(C_2H_6), $[^{13}CO]^+$, (CH_4O)
30	1.5	(C_2H_6), (CH_4O)
31	7.2	$[CH_3O]^+$, (CH_4O)
32	4.5	$[CH_4O]^+$, (CH_4O)
39	1.7	(C_3H_6)
40	42.0	$[Ar]^+$, (Ar), (C_3H_6)
41	2.5	(C_3H_6)
42	1.5	$[C_3H_6]^+$, (C_3H_6)
43	3.5	(C_3H_6O)
44	100.0	$[CO_2]^+$, (CO_2)
45	7.2	(C_3H_8O)
57	1.0	(C_3H_8O)
58	1.0	$[C_3H_6O]^+$, (C_3H_6O)
59	2.0	(C_3H_8O)

* The ions are in brackets and the initial molecules are in parentheses.

The ground-state Li_{20} cluster has an irregular structure of C_{2v} symmetry (Fig. 5, *a*), which is not a fragment of the Li geometric lattice. The calculated geometric parameters are consistent with published data.[28] On the reaction of Li_{20} with one γBL molecule, no intermediate adsorption complexes with retained γBL molecule were detected. Optimization of the Li_{20}—γBL system geometry gives directly the structure of a chemisorbed complex with C—O bond cleavage (Fig. 5, *b*) and with evolution of 66.7 kcal mol^{-1} of energy. However, intermediate complexes of such structure were localized in the study of interaction of three γBL molecules with the Li_{20} cluster (Fig. 5, *d*) with an average bond energy of 28.7 kcal mol^{-1}. These complexes are actually surface organolithium compounds, *i.e.*, γBL decomposition starts with the addition of the lithium cluster to the carbonyl double bond.

The further transformation of the structure (see Fig. 5, *b*) with deeper insertion of the carbonyl group into the surface layer of the lithium cluster (see Fig. 5, *c*) is also accompanied by heat evolution (17.9 kcal mol^{-1}). In this complex, only three methylene units do not participate in the interaction with lithium atoms. This C_3H_6 fragment of the structure can be regarded as a half-way C_3 hydrocarbon. Meanwhile, the decomposition of the complex (see Fig. 5, *c*) to give propylene and $Li_{20}CO_2$ cluster requires energy expenditure of 7.8 kcal mol^{-1}, although it is accompanied by some decrease in the free energy (−4.8 kcal mol^{-1}) as a result of increase in the translation entropy of C_3H_6. However, the one-step formation of C_3H_6 requires the 1—3-hydrogen shift to transform the trimethylene fragment to propylene, which should occur in parallel with cleavage of strong C—C and C—O bonds. Therefore, there are grounds for assuming that this reaction would have a rather high activation barrier. This conclusion is in line with the experimental fact that at the minimum possible water content (below 10^{-2}% w/w), no gassing takes place. For modeling the interaction process between water and chemisorbed γBL molecules, two successive reactions of the complex (see Fig. 5, *c*) with water molecules accompanied by C—C and C—O cleavage are considered.

At the first stage, the water molecule adds to the Li atom bound to a C atom of the adsorbed γBL molecule, the energy being reduced by 15.2 kcal mol^{-1} (see Fig. 5, *e*).

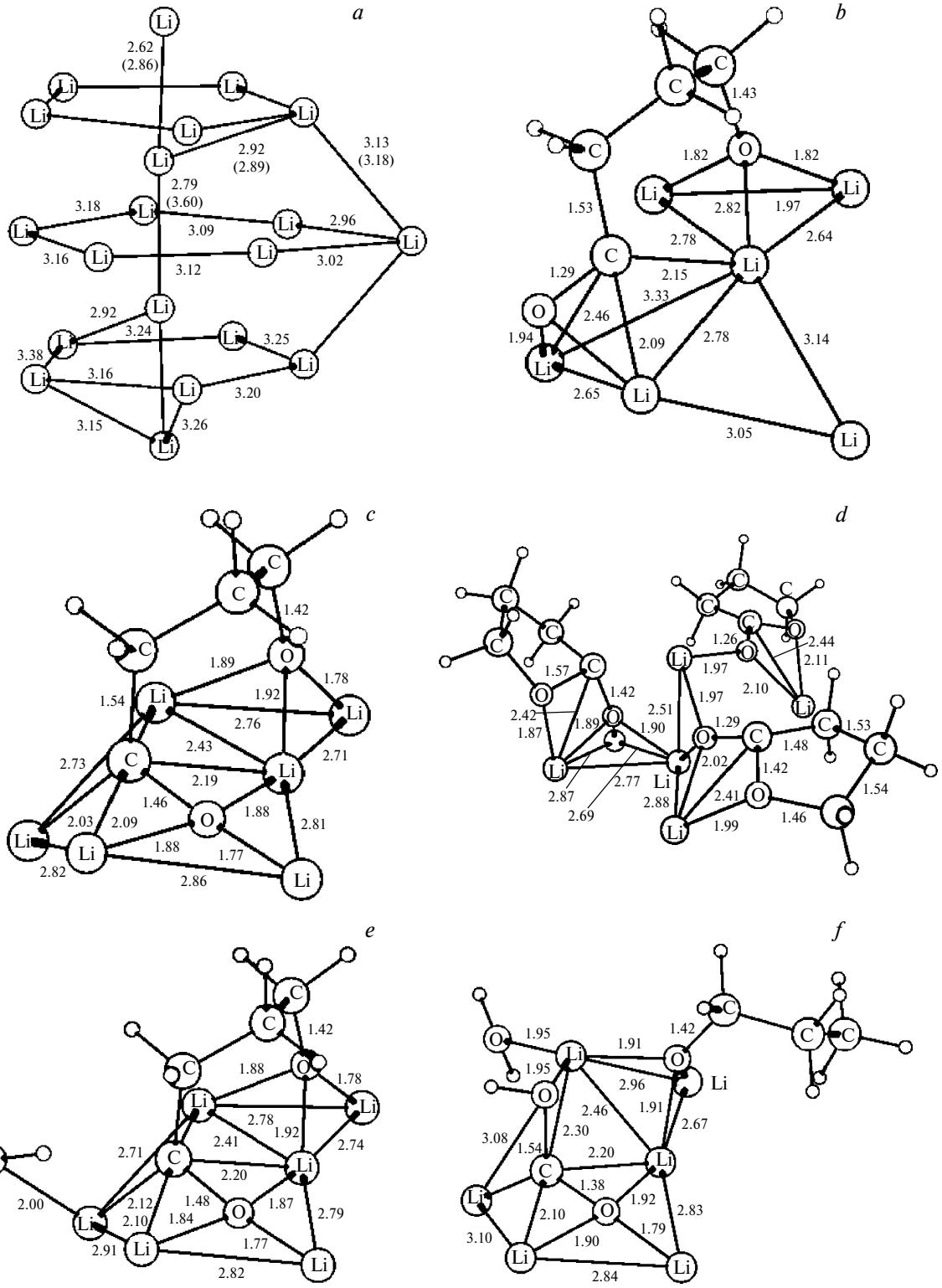

Fig. 5. Structure of the Li_{20} cluster (*a*) and fragments of the structures of $Li_{20}(\gamma BL)$ (*b*, *c*), $Li_{20}(\gamma BL)_3$ (*d*), $Li_{20}(\gamma BL)(H_2O)$ (*e*), and $Li_{20}(\gamma BL)(H_2O)_2$ (*f*) isomers; γBL is γ-butyrolactone; the bond lengths are in Å.

The next stage affords the C—H bond with simultaneous cleavage of the O—H and C—C bonds. The reaction considered is nearly thermally neutral being accompanied by evolution of 2.9 kcal mol^{-1}. This reaction involves the five-membered transition state. For this reason, the activation ener-

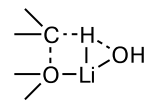

gy of this reaction should be moderate. The adsorption of the next water molecule (see Fig. 5, *f*) is also energetically favorable, resulting in the system energy decrease by 22.3 kcal mol^{-1}. Decomposition of this surface complex to give propane is accompanied by substantial energy evolution (70.3 kcal mol^{-1}). Since this reaction is highly exothermic and also involves the formation of a five-membered transition state , a relatively low activation energy is expected for this reaction. Note that the transformation of γBL molecule to propane with participation of a water molecule gives rise to chemisorbed CO_2. The products of hydrolysis of these surface complexes should contain CO_2, which was actually detected in experiments. The appearance of CO is apparently related to propylene formation. From the formal standpoint, it can be considered that in this process, two atoms migrate to the CO_2 fragment rather than the C_3 fragment of γBL. In this case, propylene, CO, and water molecule are formed. As regards the formation of alcohols detected in the mass spectra, isopropyl alcohol is the hydrated form of propylene and methanol is the product of CO reduction on the Li surface. Since hydrogen is present in the gas phase in considerable amounts, it is clear that together with the formation of H_2 from chemisorbed H atoms, the H atoms should also react with chemisorbed fragments of the γBL molecule.

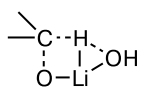

An alternative view on the mechanism of the effect of current density on gassing was also analyzed. As the current density increases, the overvoltage on the electrode increases. At high current densities, electron transfer to the γBL molecule is thermodynamically possible. To verify this assumption, electron transfer on the γBL molecule was considered. The calculated structures of the γBL$^-$ radical anion are shown in Fig. 6. The attachment of an electron with retention of the ring (see Fig. 6, *a*) requires 41.0 kcal mol^{-1}. The C—O bond cleavage affords acyclic radical anion $^{\cdot}(CH_2)_3COO^-$ with energy decrease by 24.2 kcal mol^{-1}. In the subsequent reactions, this γBL$^-$ species reacts as a primary alkyl radical. Therefore, these electron transfer reactions would give non-volatile C_3H_7COOLi salt as the final product.

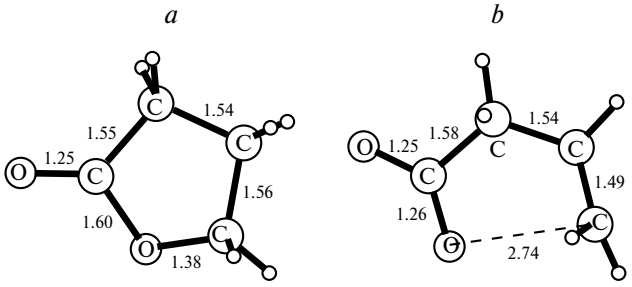

Fig. 6. Isomeric structures of the γBL radical anion; the bond lengths are in Å. For explanations, see the text.

Taking into account the solvation effects calculated in the polarizable continuum model (PCM) using the Gaussian-03 program,[29] electron transfer on the γBL molecule (see Fig. 6, *a*) induces a decrease in the free energy of solvation by 64.8 and 59.5 kcal mol^{-1} in water and in γBL, respectively. For the γBL$^-$ structure (see Fig. 6, *b*), close values, 58.4 and 58.6 kcal mol^{-1}, respectively, were found. Using the reference data on H_2 dissociation energy and H ionization potential,[30] and also the standard free energy of proton hydration (−264.0 kcal mol^{-1}),[31] the standard γBL$^-$/γBL redox potential in water was determined to be −3.29 and −2.26 V for the two isomer forms of the radical anion (see Fig. 6, *a*, *b*). For the γBL medium, the $\Delta G_{solv}(H^+)$ value is unknown but in view of the similarity of the calculated solvation energies, one should not expect considerable shift of the redox potential with respect to water.

It follows from calculated data that electron transfer to the γBL molecule requires more cathodic redox potential than the redox potential of the solvated electron equal to −2.87 V versus the standard hydrogen electrode.[32] Despite the fact that its value is sufficient for the transfer to γBL accompanied by C—O bond cleavage, this process seems unlikely for the following reason. The activation energy would be much higher in this case than that for usual electron transfer reactions, because apart from the solvent reorganization energy, an additional contribution related to bond redistribution upon γBL ring cleavage will be present.

The formation of the solvated electron in the system is less beneficial than the participation of the electron in the thermodynamically more favorable reduction of the ClO_4^- anion, as indicated by detection of $LiClO_2$ and $LiClO_3$ in the film passivating the lithium electrode surface.[3]

Even if solvent decomposition reactions by the electron transfer mechanism take place at enhanced current densities, they result in lithium salts participating in the formation of the passivating film on the electrode.

Quantum chemical modeling attests to thermodynamic favorability of the formation of surface organolithium compounds from γBL molecules.

Thus, we studied decomposition reactions of the 1 *M* $LiClO_4$ electrolyte in γBL containing 0.2% w/w of water with deposition on a pure lithium electrode and on the lithium nitride-modified electrode. The γBL solvent does not decompose at current densities of 0.5 and 1.0 mA cm^{-2} on the pure lithium electrode, while at current densities of 1.5 and 2.0 mA cm^{-2}, release of H_2, CO, and CO_2 in comparable amounts and five gaseous hydrocarbons takes place, the release rate varying upon the change in the current density. Thus for current density of 1.5 mA cm^{-2}, the gas release rate varies as: $CH_4 = C_3H_6 < C_3H_8 < C_2H_4 < C_2H_6$. For current density of 2.0 mA cm^{-2}, the variation sequence is different: $CH_4 < C_3H_6 < C_2H_4 < C_2H_6 < C_3H_8$. The use of the condensation procedure and analysis of the

condensate mass spectra demonstrated the presence of the hydrocarbons CH_4, C_2H_4, C_2H_6, and C_3H_6 and the alcohols MeOH and Pr^iOH, in addition to H_2, CO, and CO_2.

The quantum chemical calculations point to the thermodynamic utility of the formation of surface organolithium compounds from the γBL molecules.

When lithium electrode is replaced by a nitrogen-treated lithium electrode, this electrolyte does not decompose even when the current density is increased to 2.0 mA cm^{-2}. Thus, the Li_3N layer is the protective coating for lithium metal. The proposed method for modification of the lithium electrode surface by a Li_3N layer may theoretically produce a power cell that would be safe to operate at high charge currents, despite the presence of water up to 0.2% (w/w).

References

1. A. G. Demakhin, V. M. Ovsyannikov, S. M. Ponomarenko, *Elektrolitnye sistemy lithievykh KhIT* [*Electrolyte Systems of Lithium Electrochemical Power Sources*], Sarat. Univ., Saratov, 1993, 217 pp. (in Russian).
2. I. A. Kedrinskii, V. E. Dmitrenko, I. I. Grudyanov, *Litievye istochniki toka* [*Lithium Batteries*], Energoatomizdat, Moscow, 1992, 240 pp. (in Russian).
3. D. Aurbach, in *Advances in Lithium-Ion Batteries*, Eds W. A. Schalkwijk, B. Scrosati, Kluwer Academic Plenum Publishers, New York, 2002, p. 7.
4. D. Aurbach, Y. Cohen, *J. Electrochem. Soc.*, 1996, **143**, 3525.
5. D. Aurbach, *J. Electrochem. Soc.*, 1989, **136**, 1610.
6. D. Aurbach, Y. Ein-Eli, B. Markovsky, Y. Carmeli, H. Yamin, S. Luski, *Electrochimica Acta*, 1994, **39**, 2559.
7. Y. Ein-Eli, S. F. McDevitt, B. Markovsky, A. Schechter, D. Aurbach, *J. Electrochem. Soc.*, 1997, **144**, L180.
8. D. Aurbach, Y. Gofer, M. Ben-Zion, P. Aped, *J. Etectroanal. Chem.*, 1992, **339**, 451.
9. D. Aurbach, B. Markovsky, A. Schechter, Y. Ein-Eli, H. Cohen, *J. Electrochem. Soc.*, 1996, **143**, 3809.
10. D. Aurbach, B. Markovsky, K. Gamolsky, E. Levi, Y. Ein-Eli, *Electrochim. Acta*, 1999, **45**, 67.
11. D. Aurbach, O. Chusid, Y. Carmeli, M. Babai, Y. Ein-Eli, *J. Power Sources*, 1993, **43**, 47.
12. D. Aurbach, Y. Ein-Eli, O. Chusid, M. Babai, Y. Carmeli, H. Yamin, *J. Electrochem. Soc.*, 1994, **141**, 603.
13. D. Aurbach, A. Schechter, B. Markovsky, Y. Ein-Eli, V. Koch, *J. Electrochem. Soc.*, 1996, **143**, L273.
14. D. Aurbach, A. Zaban, Y. Gofer, O. Abramson, M. Ben-Zion, *J. Electrochem. Soc.*, 1995, **142**, 687.
15. D. Aurbach, M. L. Daroux, P. Faguy, E. Yeager, *J. Electrochem. Soc.*, 1988, **135**, 1863.
16. D. Aurbach, E. Granot, *Electrochim. Acta*, 1997, **42**, 697.
17. D. Aurbach, O. Chusid, I. Weissman, *Electrochim. Acta*, 1996, **41**, 747.
18. D. Aurbach, Y. Ein-Eli, *Langmuir*, 1992, **8**, 1845.
19. D. Aurbach, O. Chusid, *J. Electrochem. Soc.*, 1993, **140**, L155.
20. A. L. L´vov, *Soros. Obrazovat. Zh.* [*Soros Educational Journal*], 2001, **7**, No. 3, 45 (in Russian).
21. T. Lapp, S. Skaarup, A. Hooper, *Solid State Ionics*, 1983, **11**, 97.
22. V. F. Volynets, M. P. Volynets, *Analiticheskaya khimiya azota* [*Analytical Chemistry of Nitrogen*], Nauka, Moscow, 1977, p. 86 (in Russian).
23. R. A. Huggins, *Advanced Batteries*, *Materials Science Aspects.* Springer Science+Business Media, New York, 2009, 125.
24. P. Perdew, K. Burke, M. Ernzerhof, *Phys. Rev. Lett.*, 1996, **77**, 3865.
25. D. N. Laikov, *Chem. Phys. Lett.*, 1997, **281**, 151.
26. B. Temelso, D. Sherrill, *J. Chem. Phys.*, 2005, **122**, 064315.
27. R. J. Papoular, N. Allouchi, A. Chagnes, A. Dzyabchenko, B. Carre, D. Lemordant, V. Agafonov, *Acta Crystallogr., Sect. B*, 2005, **61**, 312.
28. J. K. V. Jovan, R. G. Shridhar, *J. Chem. Phys.*, 2008, **129**, 164314.
29. M. J. Frisch, G. W. Trucks, H. B. Schlegel, G. E. Scuseria, M. A. Robb, J. R. Cheeseman, J. A. Montgomery, Jr., T. Vreven, K. N. Kudin, J. C. Burant, J. M. Millam, S. S. Iyengar, J. Tomasi, V. Barone, B. Mennucci, M. Cossi, G. Scalmani, N. Rega, G. A. Petersson, H. Nakatsuji, M. Hada, M. Ehara, K. Toyota, R. Fukuda, J. Hasegawa, M. Ishida, T. Nakajima, Y. Honda, O. Kitao, H. Nakai, M. Klene, X. Li, J. E. Knox, H. P. Hratchian, J. B. Cross, C. Adamo, J. Jaramillo, R. Gomperts, R. E. Stratmann, O. Yazyev, A. J. Austin, R. Cammi, C. Pomelli, J. W. Ochterski, P. Y. Ayala, K. Morokuma, G. A. Voth, P. Salvador, J. J. Dannenberg, V. G. Zakrzewski, S. Dapprich, A. D. Daniels, M. C. Strain, O. Farkas, D. K. Malick, A. D. Rabuck, K. Raghavachari, J. B. Foresman, J. V. Ortiz, Q. Cui, A. G. Baboul, S. Clifford, J. Cioslowski, B. B. Stefanov, G. Liu, A. Liashenko, P. Piskorz, I. Komaromi, R. L. Martin, D. J. Fox, T. Keith, M. A. Al-Laham, C. Y. Peng, A. Nanayakkara, M. Challacombe, P. M. W. Gill, B. Johnson, W. Chen, M. W. Wong, C. Gonzalez, J. A. Pople, *GAUSSIAN 03*, *Revision C.02*, Gaussian, Inc., Wallingford (CT), 2004.
30. L. V. Gurvich, I. V. Veits, V. A. Medvedev, *Termodinamicheskie svoistva individual´nykh veshchestv*, Spravochnoe izdanie [*Thermodynamic Properties of Individual Compounds. A Reference Book*], V. **1**, Book 2, Nauka, Moscow, 1978, 328 pp. (in Russian).
31. M. D. Tissandier, K. A. Cowen, W. Y. Feng, E. Gundlach, M. H. Cohen, A. D. Earhart, J. V. Coe, Jr., T. R. Tuttle, *J. Phys. Chem. A*, 1998, **102**, 7787.
32. A. K. Pikaev, *Sovremennaya radiatsionnaya khimiya* [*Modern Radiation Chemistry*], Nauka, Moscow, 1986, 440 pp. (in Russian).

Recevied May 12, 2009;
in revised December 10, 2009